Contents lists available at ScienceDirect

Ecological Modelling

journal homepage: www.elsevier.com/locate/ecolmodel

Simulating microbial denitrification with EPIC: Model description and evaluation

R. César Izaurralde [a,b,*], William B. McGill [c], Jimmy R. Williams [b], Curtis D. Jones [a], Robert P. Link [d], David H. Manowitz [d], D. Elisabeth Schwab [e], Xuesong Zhang [d], G. Philip Robertson [f,g,h], Neville Millar [f,g,h]

[a] Department of Geographical Sciences, University of Maryland, 2181 LeFrak Hall, College Park, MD 20742, USA
[b] Texas Agri-Life Research and Extension, Texas A&M University, 720 East Blacklands Road, Temple, TX 76502, USA
[c] Ecosystem Science and Management, University of Northern British Columbia, 3333 University Way, Prince George, BC, V2N 4Z9, Canada
[d] Joint Global Change Research Institute, Pacific Northwest National Laboratory/University of Maryland, 5825 University Research Ct., Suite 305, College Park, MD 20740, USA
[e] Department of Economic and Social Sciences, Institute of Sustainable Economic Development, University of Natural Resources and Applied Life Sciences, Guttenberghaus, Feistmantelstrasse 4, A-1180 Vienna, Austria
[f] Department of Plant, Soil, and Microbial Sciences, Michigan State University, East Lansing, MI 48824, USA
[g] Great Lakes Bioenergy Research Center, Michigan State University, East Lansing, MI 48824, USA
[h] W.K Kellogg Biological Station, Michigan State University, Hickory Corners, MI 49060, USA

ARTICLE INFO

ABSTRACT

Microbial denitrification occurs in anaerobic soil microsites and aquatic environments leading to production of N_2O and N_2 gases, which eventually escape to the atmosphere. Atmospheric concentrations of N_2O have been on the rise since the beginning of the industrial revolution due to large-scale manipulations of the N cycle in managed ecosystems, especially the use of synthetic nitrogenous fertilizer. Here we document and test a microbial denitrification model identified as IMWJ and implemented as a submodel in the EPIC terrestrial ecosystem model. The IMWJ model is resolved on an hourly time step using the concept that C oxidation releases electrons that drive a demand for electron acceptors such as O_2 and oxides of N (NO_3^-, NO_2^-, and N_2O). A spherical diffusion approach is used to describe O_2 transport to microbial surfaces while a cylindrical diffusion method is employed to depict O_2 transport to root surfaces. Oxygen uptake by microbes and roots is described with Michaelis-Menten kinetic equations. If insufficient O_2 is present to accept all electrons generated, the deficit for electron acceptors may be met by oxides of nitrogen, if available. The movement of O_2, CO_2 and N_2O through the soil profile is modeled using the gas transport equation solved on hourly or sub-hourly time steps. Bubbling equations also move N_2O and N_2 through the liquid phase to the soil surface under highly anaerobic conditions. We used results from a 2-yr field experiment conducted in 2007 and 2008 at a field site in southwest Michigan to test the ability of EPIC, with the IMWJ option, to capture the non-linear response of N_2O fluxes as a function of increasing rates of N application to maize [*Zea mays* L.]. Nitrous oxide flux, soil inorganic N, and ancillary data from 2007 were used for EPIC calibration while 2008 data were used for independent model validation. Overall, EPIC reproduced well the timing and magnitude of N_2O fluxes and NO_3^- mass in surficial soil layers after N fertilization. Although similar in magnitude, daily and cumulative simulated N_2O fluxes followed a linear trend instead of the observed exponential trend. Further model testing of EPIC + IMWJ, alone or in ensembles with other models, using data from comprehensive experiments will be essential to discover areas of model improvement and increase the accuracy of N_2O predictions under a wide range of environmental conditions.

1. Introduction

Denitrification is the biological reduction of NO_3^- or NO_2^- to the gases N_2O and N_2 (Saggar et al., 2013a,b; Robertson and Groffman, 2015). Although reduction of NO_3^- to NO_2^- has been reported to occur in oxic environments (Roco et al., 2016) denitrification is

* Corresponding author at: Department of Geographical Sciences, University of Maryland, 2181 LeFrak Hall, College Park, MD 20742, USA.
E-mail address: cizaurra@umd.edu (R.C. Izaurralde).

typically a respiratory process in which NO_3^- (or NO_2^-) replaces oxygen as terminal electron acceptor in facultative anaerobes. Such organisms are capable of extracting energy for their metabolism by coupling oxidation of reduced C or reduced S to reduction of oxides of N (e.g., NO_3^-, NO_2^-) yielding variable proportions of N_2O and N_2 (Conrad, 1996; Saggar et al., 2013a,b). Nitrous oxide is a potent greenhouse gas (Rodhe, 1990) that also depletes the protective layer of stratospheric O_3 (Crutzen, 1970). Atmospheric concentrations of N_2O have been rising since the beginning of the industrial revolution due to large-scale manipulations of the N cycle in managed ecosystems, especially due to use of synthetic nitrogenous fertilizer (Davidson, 2009; Khalil et al., 2002).

Current atmospheric N_2O concentrations of 330 ppb are $\sim$20% larger than those present in the pre-industrial era and during the last decades have been increasing at an annual rate of 0.73 ± 0.03 ppb yr^{-1} (Ciais et al., 2014). Soils produce $\sim$70% of the N_2O flux to the atmosphere mainly through microbial denitrification under anaerobic conditions and, to a lesser extent, through ammonia oxidation and nitrifier denitrification that occur during nitrification under partially anaerobic conditions (Conrad, 1996; Kool et al., 2011; Robertson and Tiedje, 1987; Zhu et al., 2013). Many biophysical factors control the production of N_2O in soils including those directly affected by management such as levels of NO_3^-, O_2 availability, soil water content, and soil temperature (Mosier et al., 1996).

There is a need—and significant potential—to reduce N_2O emissions from managed ecosystems (Khalil et al., 2002; Mosier et al., 1996; Robertson et al., 2000; Smith et al., 2008). Reduced N_2O emissions can be achieved through improved N management by combining organic and inorganic sources, optimizing rate, time, and placement of fertilizer application, and—in some cases—by using nitrification inhibitors (Smith et al., 2008). In order to evaluate N_2O emissions reductions from managed soils, the Intergovernmental Panel on Climate Change (IPCC) has developed a 3-tier approach that includes both direct and indirect emissions of N_2O (De Klein et al., 2006). Following this approach, direct N_2O emissions primarily arise from application of synthetic N fertilizers, organic N amendments, and management of organic soils. In managed soils, indirect N_2O emissions arise from N lost to downwind and downstream ecosystems as NH_3 and NO_x, redeposited as NH_4^+ and NO_3^-, and as N lost via leaching and runoff (Robertson et al., 2013).

The three tiers range in complexity (De Klein et al., 2006). In Tier 1, a fertilizer-based emission factor is used to estimate direct N_2O emissions from managed soils. In Tier 2, more detailed—country specific—emission factors are used to estimate N_2O emissions. Finally, the Tier 3 method is based on modeling or measurement approaches. Process-based field-scale N_2O simulation models are deemed useful in the Tier 3 approach because they can help identify the soil and environmental variables responsible for N_2O emissions and allow for the projection of these N_2O emissions to regional and country scales (Chen et al., 2008). Simulation of N_2O emissions, however, carry uncertainties associated with model structure, model parameterization, accuracy of input data, and resolution of spatial and temporal scales. For example, Nol et al. (2010) used Monte Carlo uncertainty propagation analysis to quantify uncertainties of modeled N_2O emissions caused by model input uncertainty at point and landscape scales. Nitrous oxide emission at landscape scale averaged 20.5 ± 10.7 kg N_2O-N ha^{-1} yr^{-1}, producing a relative uncertainty of 52%. At point scale, the relative error averaged 78%, suggesting that upscaling decreases uncertainty. The results confirmed the influence of spatial scale on the uncertainty of modeled results.

Several terrestrial ecosystem models are available to estimate N_2O emissions from managed and unmanaged ecosystems at site, regional, and national scales. They vary in level of resolution, degree of connection to the C cycle and connection between the biological and physical components of the system being modeled (Chen et al., 2008). Three examples of such models include DNDC (Li et al., 1992, 1996), *ecosys* (Grant et al., 1993a, 1993b; Grant and Pattey, 1999), and DayCent (Del Grosso et al., 2000, 2006; Parton et al., 1996). Comparisons of N_2O dynamics (Frolking et al., 1998; Li et al., 2005) and simulation approaches (Chen et al., 2008) employed by N_2O models emphasize the importance of accurate simulation of soil water content and its appropriate linking with denitrification and N_2O flux.
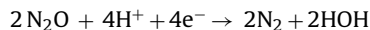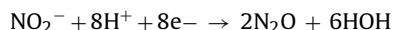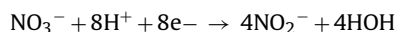
Modeling soil water dynamics is a strength of the Environmental Policy Integrated Climate (EPIC) terrestrial ecosystem model (Williams et al., 1984). Developed originally to model the relationship between erosion and soil productivity, the EPIC model has evolved into a comprehensive and widely used terrestrial ecosystem model (Williams et al., 2008). Our objectives here are to: (a) document a process-based microbial denitrification submodel implemented in EPIC thus adding to two other empirically-based (EPIC-specific) options to simulate denitrification (Williams, 1990); and, (b) test the new microbial denitrification model for its ability to reproduce experimental data (Hoben et al., 2011) exhibiting a non-linear response of N_2O fluxes to incremental rates of N application.

The process-based microbial denitrification model documented and tested here —IMWJ— quantifies microbial denitrification in soils under O_2-limiting conditions. Daily C oxidation quantified in the C model of EPIC (Izaurralde et al., 2006) releases electrons, which are accepted by O_2 under aerobic conditions. Oxygen uptake by microbes and roots is described with Michaelis-Menten kinetic equations. If O_2 is insufficient, then the deficit for electron acceptors may be met by oxides of N (NO_3^-, NO_2^-, and N_2O). When denitrification occurs, there is an adjustment of C decomposition based on the ratio of actual vs. potential electrons accepted by O_2 and oxides of N. The movement of O_2, CO_2, and N_2O through the soil profile is modeled using the gas transport equation solved with an adaptive variable time step.

2. Description of the denitrification submodel in EPIC

2.1. Conceptual framework and model overview

The version of EPIC containing the denitrification submodel described and tested herein is identified as EPIC1704. The denitrification model presented here is identified as the IMWJ (Izaurralde, McGill, Williams, and Jones) denitrification option in EPIC. The connection between main IMWJ subroutines and relevant EPIC subroutines is shown in Appendix 6.1. Microbial decomposition of soil organic matter and respiration by plant roots results in oxidation of C (Fig. 1). Such oxidation produces electrons, typically carried within the cell as $NADH + H^+$, for which there must be an acceptor to allow decomposition or respiration to produce CO_2. Normally O_2 is the acceptor but in cases of O_2 deficiency electrons are transferred to N in NO_3^- to yield NO_2^- and thence N_2O and N_2 through denitrification as shown in the following equations:

$$CH_2O + 5HOH \rightarrow 5CO_2 + 20H^+ + 20e^-$$

$$NO_3^- + 8H^+ + 8e^- \rightarrow 4NO_2^- + 4HOH$$

$$NO_2^- + 8H^+ + 8e^- \rightarrow 2N_2O + 6HOH$$

$$2N_2O + 4H^+ + 4e^- \rightarrow 2N_2 + 2HOH$$

Overall: $5CH_2O + 4NO_3^- + 4H^+ \rightarrow 5CO_2 + 2N_2 + 7HOH + energy$

The potential supply of electrons is calculated based on moisture content and temperature coupled with the nature and supply
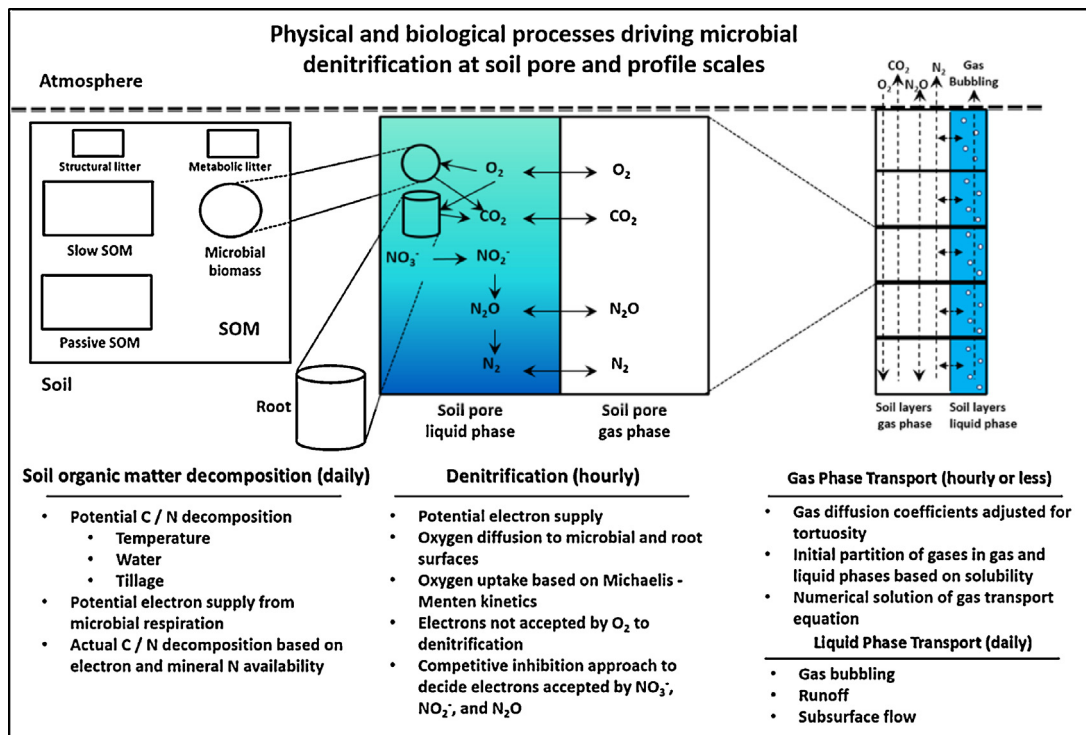
Fig. 1. Diagram of denitrification in EPIC.

of available substrates (Izaurralde et al., 2006). Electrons are first passed to O_2, based on O_2 concentration at the surface of both soil microorganisms and plant roots to form CO_2. Michaelis-Menten uptake kinetic equations are used to evaluate electron transfer to O_2.

If the potential supply of electrons exceeds those accepted by O_2, and if oxides of N (NO_3^-, NO_2^- or N_2O) are present then electrons are passed to oxides of N (to emulate denitrification). Uptake of electrons by organisms reducing oxides of N is quantified via Michaelis-Menten kinetics (Grant and Pattey, 1999). Complete reduction of 1 mol of NO_3^- consumes 5 mol of electrons, compared to 3 mol of electrons for 1 mol of NO_2^- and 1 mol of electrons per mole of N_2O. Accordingly, the concentrations of each of the oxides of N are weighted to account for the variation in numbers of moles of electrons that each species accepts. The energy gain from reducing NO_3^- exceeds that from reducing NO_2^-, which exceeds that from reducing N_2O. Consequently, the Michaelis-Menten expression contains terms for competitive inhibition such that NO_3^- inhibits reduction of NO_2^-, and both inhibit reduction of N_2O.

A feedback mechanism based on electron acceptors controls decomposition. If potential supply of electrons is matched by the total accepted by O_2 plus oxides of N, then, decomposition equals potential decomposition, variables are updated and calculations start again for the next day. If, however, potential supply of electrons exceeds those accepted by O_2 plus oxides of N, then actual decomposition is reduced sufficiently such that total electron supply equals total electrons accepted by O_2 plus oxides of N.

The simultaneous diffusion of four gases (O_2, CO_2 N_2O, and N_2) is modeled using the gas transport equation (Šimůnek and Suarez, 1993). Within each day, each gas is transferred within the gas phase of the soil profile and between the soil surface and the atmosphere above. The profile is divided into computational layers of equal thickness. Properties of the soil profile layers are interpolated among the computational layers. Gas diffusion within the gaseous-phase of the soil profile is calculated using the Crank-Nicolson procedure (Crank and Nicolson, 1996) as default although

the implicit and explicit procedures are included as options. Like the implicit and explicit methods, the Crank-Nicolson procedure is a finite difference method for solving numerically the heat and other partial differential equations. Gas diffusivity in soil is modified from air diffusivity to account for tortuosity and water-filled pore space according the Millington-Quirk approach (Millington and Quirk, 1961). The layer beneath the soil profile is considered a zero-flux boundary, while the atmospheric gas concentrations above the soil profile are fixed at atmospheric levels. Each gas is redistributed hourly between gas and liquid phases using Henry's Law. Flux of each gas across the soil-atmosphere plane is calculated from the surface boundary term of the diffusion equation at each diffusion time step and is accumulated into daily fluxes. Gaseous flow through bubbling allows movement of dissolved gases through the liquid phase to the soil surface when aggregate partial pressures exceed atmospheric pressure, which typically only occurs under highly anaerobic conditions.

2.2. Integrating denitrification with soil C dynamics and gas exchange (See Appendix 6.2. for definition of names, values, and units of selected variables and parameters used in this section)

In EPIC-IMWJ, electron supply is generated via microbial and root respiration. Oxidation of C by microbial respiration (RSPC, mol e$^-$ m^{-2} h^{-1}) liberates electrons (e$^-$), and the flux of e$^-$ (ES$_M$; mol e$^-$ m^{-2} h^{-1}) drives the demand for e$^-$ acceptors.

$$ES_M = RSPC\frac{0.1}{72} \tag{1}$$

Dimensions: $RSPC\frac{kgC}{had}\frac{10^3 gC}{kgC}\frac{10^{-4}ha}{m^2}\frac{1d}{24h}\frac{1molC}{12gC}\frac{4mole^-}{molC} = RSPC\frac{0.1}{72}$ mol e$^-$ m^{-2} h^{-1}.

Like microbial respiration, root respiration oxidizes C for growth and maintenance, thereby generating e$^-$ (ES$_R$; mol e$^-$ m^{-2} h^{-1}). Growth respiration (RRG) is calculated as a function (RRF; dimen-

sionless) of the increase in root mass (ΔRWT) per day based on the carbon allocated to the root each day (CA).

$$RRG = RRF \times CA \tag{2}$$

Dimensions:$= \frac{kgDM}{had} \cdot \frac{0.42kgC}{kgDM} \cdot \frac{10^3 gC}{kgC} \cdot \frac{10^{-4}ha}{m^2} \cdot \frac{1d}{24h} \cdot \frac{1molC}{12gC} \cdot \frac{4mole^-}{molC}$

$= RRFxCAx\frac{0.168}{288} \text{mol } e^- m^2 h^{-1}.$

In contrast, maintenance respiration (RRM; $\text{mol } e^- \, m^{-2} \, h^{-1}$) is treated as a function (RMF; d^{-1}) of root mass (RWT; $kg \, ha^{-1}$).

$$RRM = RMF \times RWT \times \frac{0.168}{288} \text{mol } e^- m^{-2} h^{-1}. \tag{3}$$

Total root respiration (ES_R; $\text{mol } e^- \, m^{-2} \, h^{-1}$) is the sum of maintenance and growth respiration.

$$ESR = \frac{0.168}{288}(RRF \times CA + RRM \times RWT) \tag{4}$$

Diffusion transports O_2 for respiration (Campbell, 1985; Scott, 2000). In the case of microbial respiration, we considered diffusion to a sphere· and calculated the conductance (K) as:

$$K = 4\pi D_{sO2} \frac{r_1 r_2}{r_1 - r_2} \tag{5}$$

For the case of roots, the diffusion occurs in cylindrical coordinates and K is:

$$K = \frac{2\pi D_{sO2}}{ln\left(r_2/r_1\right)} \tag{6}$$

Where D_{sO2} = Diffusion coefficient of O_2 in soil water (at $20\,^\circ C = 7.2 \times 10^{-6} \, m^2 \, h^{-1}$); r_1 = radius of microbe or root (m); and r_2 = radius of water film plus microbe or root (m).

The units of K vary with the coordinate system used. For spherical systems (soil aggregates or colonies of microorganisms), the units of K are $m^3 \, s^{-1}$ and the flux (j) is per sphere. For a cylindrical system, the units of K are $m^2 \, s^{-1}$ and j is per meter of (root) length.

Gas transport to microbial surfaces is modeled with the following equation (Grant and Pattey, 1999):

$$EA_{O2m} = 4 \cdot \pi \cdot n \cdot MBC \cdot 10^{-4} \cdot D_{sO2} \cdot \frac{(dm \cdot dw)}{(dw - dm)}([O_{2s}] - [O_{2m}])\frac{4}{32} \tag{7}$$

Dimensions: $EA_{O2m} = \frac{1}{kgC} \cdot \frac{kgC}{ha} \cdot \frac{ha}{m^2} \cdot \frac{m^2}{h} \cdot \frac{m.m}{m} \cdot \frac{gO_2}{m^3} \cdot \frac{molO_2}{gO_2} \cdot \frac{mole^-}{molO_2} = \frac{mole^-}{hm^2}$

Where EA_{O2m} = Electrons accepted by O_2 during microbial respiration (mol $e^- \, m^{-2} \, h^{-1}$); MBC = Microbial biomass C (kg C ha^{-1}) that is active (see Additional Modification section below); D_{sO2} = as defined in (6); dm = radius of microbe (r_1 in (5); 10^{-6} m); dw = radius of water film plus microbe (r_2 in (5); as calculated below in (11), m); $[O_{2s}]$ = concentration of O_2 in the soil water film as calculated in EPIC using gas transport and convective flow (g $O_2 \, m^{-3}$ soil water); n = number of microbes per kg biomass C; and $[O_{2m}]$ = concentration of O_2 at surface of microbe (g $O_2 \, m^{-3}$ soil water) as calculated below in (17).

The number of microbes per kg biomass C (n) is calculated based on spherical organisms as:

$$\frac{kgC}{cell} = \frac{4}{3} \cdot \pi r^3 \cdot \rho_w \cdot F_{dm} \cdot C_{dm} \cdot \frac{kg}{Mg} \tag{8}$$

And $n = \frac{1}{kgC/cell} = 2.58368 \times 10^{15}$ (9)

Where r = radius of microbes (10^{-6} m); ρ_w = wet density of microbes (1.1 Mg m^{-3}); F_{dm} = Fraction of dry matter (0.2); and, C_{dm} = Carbon fraction in dry matter (0.42).

The diffusion coefficient of O_2 in soil water (D_{sO2}) is adjusted for temperature.

$$D_{sO2} = D_{sb}O_2 \cdot \left(\frac{T + 273.15}{20 + 273.15}\right)^6 \tag{10}$$

Where $D_{sb}O_2$ = base diffusion coefficient ($7.2 \times 10^{-6} \, m^2 \, h^{-1}$) at $20\,^\circ C$, (p. 6–194), (Lide, 2001)).

Two options are available in EPIC to estimate water film thickness (DW). The first method, called water-potential method, is based on relationships among volumetric water content (VWC), total porosity (TPOR) and water potential (WP). The second, called the accessible-water method, is based on accessible pore volume and accessible water volume based on diameters of pores relative to microbes. Details of these two methods are given in SI Appendix 6.3. Calculation of DW.

Using the water potential method, which is simpler:

$$dw = dm + 8x10^{-6} \cdot WP^{-0.945703126} \tag{11}$$

Where dw = radius of water film plus microbe (m); dm = radius of microbe as in (7); and, WP = water potential (bars).

2.3. Active/passive biomass

In this paper, we use "active" instead of "total" microbial biomass in the calculation of O_2 transport to microbial surfaces (see Eq. (7) above). To implement the modification, we follow the recent approach of Wang et al. (2014) to represent dormant and active microbial dynamics, which is based on microbial physiological states as well as parameters specifying maximum specific growth and maintenance rates of active microbes and the ratio of dormant to active maintenance rates.

2.4. Oxygen transport and uptake

Transport of O_2 to roots through the soil solution on an hourly basis is a product of conductance and change in $[O_2]$. Conductance to roots (K_R) within a soil layer can be calculated as:

$$K_R = \frac{2\pi D_{sO2}}{ln\left(r_2/r_1\right)}\frac{m^2}{h} \cdot \frac{2x10^5 mroot}{kgroot} \cdot \frac{kgroot}{ha} \cdot \frac{10^{-4}ha}{m^2} = \frac{125.66 \cdot D_{sO2} \cdot RWT}{ln\left(r_2/r_1\right)}\frac{m}{h} \tag{12}$$

The value 2×10^5 m root/kg root is an average for winter wheat roots obtained from (Wild, 1988) (p. 125, Table 4.3). Other representative values are: $10^5 \, m \, kg^{-1}$ for maize and soybean and $2.5 \times 10^5 \, m \, kg^{-1}$ for sorghum.

Electrons accepted by O_2 during root respiration (mol $e^- \, m^{-2} \, h^{-1}$) is the product of K_R and the difference in O_2 concentrations in the soil solution and at the root surface:

$$EA_{O2R} = K_R([O_{2s}] - [O_{2r}]) \tag{13}$$

Which expands to:

$$EA_{O2R} = \frac{125.66 \cdot D_{SO2} \cdot RWT}{ln\left(r_2/r_1\right)}([O_{2s}] - [O_{2r}])\frac{4}{32} \tag{14}$$

Where EA_{O2R} = Electrons accepted by O_2 during root respiration (mol $e^- \, m^{-2} \, h^{-1}$); RWT is as defined for (3); D_{SO2} is as defined for (5), (6); O_{2S} is as defined for (7); O_{2r} = O_2 concentration at the surface of roots (g $O_2 \, m^{-3}$ soil water); r_1 = radius of plant roots (set at 0.001 m); and, r_2 = radius of soil water film thickness plus plant roots (m).

Dimensions: $EA_{O2R} = \frac{m}{h} \cdot \frac{go_2}{m^3} \cdot \frac{molo_2}{go_2} \cdot \frac{mole^-}{molo_2} = \frac{mole^-}{m^2 h}$

Analogous to dw, values for r_2 are calculated as:

$$r_2 = r_1 + 8x10^{-6} \cdot WP^{-0.945703126} \tag{15}$$

Microbialuptakeismodifiedfrom Grant and Pattey (1999)

$$EA_{O2m} = ES_M \cdot \frac{[O_{2m}]}{([O_{2m}] + K_{O2})} \quad (16)$$

Where EA_{O2m}, $[O_{2m}]$, and $[O_{2s}]$ are as defined for (7); ES_M as defined for (1); and, K_{O2} = half-saturation value for O_2 uptake (g O_2 m^{-3} soil water).

Dimensions: $EA_{O2m} = \frac{mole^-}{m^2h} \frac{gm^{-3}}{gm^{-3}} = \frac{mole^-}{m^2h}$

Uptake of O_2 by microbes or roots requires O_2 to travel from the gas phase through the liquid phase to the uptake surface. Transport is inversely proportional and uptake directly proportional to $[O_2]$ at the surface of microbe $[O_{2m}]$ or root $[O_{2r}]$. The challenge is to find the concentration at the surface of microbes or roots, which is a function of potential rate of uptake and rate of transport to the organism surface.

Since Eqs. (16) and (7) for EA_{O2m} are equivalent, they are equated, rearranged into a quadratic expression (see SI Appendix 6.4. Derivation of method to calculate concentration of O_2 at the surface of microbial cells) and solved for O_{2m}.

$$[O_{2m}] = \frac{-B + \sqrt{B^2 - 4 \cdot A \cdot C}}{2A} \quad (17)$$

The positive solution is used because A is negative. Where, $A = -K_T$; $B = (K_T \cdot [O_{2s}] - K_T \cdot K_{O2} - ES_M)$; $C = K_T \cdot K_{O2} \cdot [O_{2s}]$; and, $K_T = 4 \cdot \pi \cdot n \cdot MBC \cdot 10^{-4} \cdot D_{sO2} \frac{(dm \cdot dw)}{(dw - dm)} \frac{4}{32}$

The value of O_{2m} is then used to calculate the value of EA_{O2m}. As with microbes, uptake of O_2 by roots is calculated as:

$$EA_{O2R} = ES_R \cdot \frac{[O_{2R}]}{([O_{2R}] + K_{O2R})} \quad (18)$$

Eqs. (13) and (18) are equivalent and are used to solve for $[O_{2r}]$ as in (19) using:

$$A = -K_R; B = (K_R \cdot [O_{2s}] - K_R \cdot K_{O2R} - ES_R); C = K_R \cdot$$

$$K_{O2R} \cdot [O_{2s}]; and K_R = \frac{125.66 \cdot D_{sO2} \cdot RWT}{ln\left(r_2/r_1\right)} \frac{m}{h}$$

$$[O_{2R}] = \frac{-B + \sqrt{B^2 - 4 \cdot A \cdot C}}{2A} \text{ g } O_2 \text{ m}^{-3} \quad (19)$$

The value of O_{2R} from (19) is used in (18) to solve for EA_{O2R} (mol e$^-$ m^{-2} h^{-1}). The sum of electrons accepted by O_2 during microbial and root respiration (EA_{O2SUM}) is then the sum of equations (16) and (18). The electrons not accepted by O_2, and hence available for denitrification, (ESD), is the difference between supply (Eqs. (1) (ES_M) plus (4) (ES_R)) and accepted electrons. It is calculated as:

$$ESD = FD \cdot (ES_M + ES_R - EA_{O2SUM}) \quad (20)$$

The term FD (coded as PRMT97, Table 1) accounts for the fact that microbial growth rate under anaerobic conditions is slower than under aerobic conditions. Hence, ESD is the theoretical deficit.

2.5. Competition for electrons among oxides of N

Oxides of N compete for electrons and as modeled exhibit competitive inhibition behavior. Competition is simulated by calculating a competitive inhibition-weighting factor for each oxide, and summing them for all oxides. The dimensionless weighting factors

are WN5 for NO_3^- reduction; WN3 for NO_2^- reduction and WN1 for N_2O reduction:

$$WN5 = 2 \cdot \frac{\left[NO_3^-\right]}{XKN5 + [NO_3^-]} \quad (21)$$

$$WN3 = 1 \cdot \frac{\left[NO_2^-\right]}{XKN3 \cdot \left(1 + \frac{\left[NO_3^-\right]}{XKN5}\right) + [NO_2^-]} \quad (22)$$

$$WN1 = 1 \cdot \frac{[N_2O]}{XKN1 \cdot \left(1 + \frac{\left[NO_2^-\right]}{XKN3}\right) + [N_2O]} \quad (23)$$

Ranges of values for XKN5, XKN3, and XKN1 are provided in Table 1. All variables on the right side of the equations have units of g m^{-3}. The rates of electron acceptance during denitrification (mol e$^-$ m^{-2} h^{-1}) are calculated as:

$$EAN5 = ESD \cdot \frac{WN5}{(WN5 + WN3 + WN1)}, EAN5 < WNO3 \cdot \left(\frac{0.1}{7}\right)/dt \quad (24)$$

$$EAN5 = WNO3 \cdot \left(\frac{0.1}{7}\right)/dt \quad (25)$$

$$EAN3 = ESD \cdot \frac{WN3}{(WN5 + WN3 + WN1)}, EAN3 < WNO2 \cdot \left(\frac{0.1}{7}\right)/dt \quad (26)$$

$$EAN3 = WNO2 \cdot \left(\frac{0.1}{7}\right)/dt \quad (27)$$

$$EAN1 = ESD \cdot \frac{WN1}{(WN5 + WN3 + WN1)}, EAN1 < WNO2 \cdot \left(\frac{0.1}{14}\right)/dt \quad (28)$$

$$EAN1 = WN2O \cdot \left(\frac{0.1}{14}\right)/dt \quad (29)$$

Dimensions:
EAN(5, 3, 1) = mol e$^-$ m^{-2} h^{-1}; WNO3 = kg N ha^{-1}; dt = 1 h.
For NO_3^-:
EAN5 = $WNO3 \cdot \frac{kgN}{ha} \cdot \frac{1}{h} \cdot \frac{2mol.e-}{14gN} \cdot \frac{103gN}{kgN} \cdot \frac{10-4ha}{m2} = WNO3 \cdot$
$\left(\frac{0.1}{7}\right) \frac{mol.e-}{m2h}$
Similarly, for N_2O:
EAN1 = $WN2O \cdot \frac{kgN}{ha} \cdot \frac{1}{h} \cdot \frac{2mol.e-}{28gN} \cdot \frac{103gN}{kgN} \cdot \frac{10-4ha}{m2} = WN2O \cdot$
$\left(\frac{0.1}{14}\right) \frac{mol.e-}{m2h}$
Then, the total number of electrons accepted by O_2 and oxides of N during an hour and for a given layer is calculated as:

$$EA = EA + EAO2M + EAO2R + EAN5 + EAN3 + EAN1 \quad (30)$$

Once daily EA is calculated for a soil layer, a ratio between accepted and supplied electrons (EAR) is calculated and used to constrain decomposition. By definition, EAR ranges between 0 and 1. Finally, the model calculates the amount of O_2 consumed, computes the quantities of CO_2, N_2O and N_2 generated, and updates the mass remaining as NO_3, NO_2, and N_2O.

2.6. Urea hydrolysis, nitrification, and nitrifier denitrification

Urea hydrolysis from fertilizer urea is modeled in the subroutine UREAHYDROLYSIS following (Godwin and Jones, 1991). The

Table 1
Pertinent model options and parameter values to run the IMWJ denitrification option in EPIC1704.

EPIC file	Variable name	Option	Definition	Unit	Value (range)
EPICCONT	IDN	3	IMWJ denitrification submodel (Pore-water thickness method 1)	–	–
	IDN	4	IMWJ denitrification submodel (Pore-water thickness method 2)	–	–
	IPRK	1	Slug-flow approach	–	–
	IPRK	2	Richard's flow approach	–	–
	DZ		Layer thickness for solution of gas transport equation	m	0.1–0.2
SITEFILE	DTG		Time interval for solution of gas transport equation	h	0.5–1.0
SOILFILE	CGO2		Initial value of O_2 concentration in gas phase	$g\,m^{-3}$	110–275
	CGCO2		Initial value of CO_2 concentration in gas phase	$g\,m^{-3}$	0.2–1.2
	CGN2O		Initial value of N_2O concentration in gas phase	$g\,m^{-3}$	0.004–0.01
PARM1704	PRMT82		Microbial N:C ratio at which N immobilization is maximum	–	0.025–0.075
	PRMT83		Microbial N:C ratio at which N immobilization ceases	–	0.2–0.04
	PRMT84		Specific base rate for ammonification	d^{-1}	0.2–0.4
	PRMT85		Microbial N:C ratio at which ammonification ceases	–	0.025–0.075
	PRMT86		Microbial N:C ratio at which ammonification is maximum	–	0.2–0.04
	PRMT87		Maximum rate of nitrogen uptake during immobilization	$gN\,gC^{-1}\,d^{-1}$	0.2–0.5
	PRMT88		Half saturation constant for ammonia immobilization	$mg\,N\,L^{-1}$	10.0–20.0
	PRMT89		Half saturation constant for nitrite immobilization	$mg\,N\,L^{-1}$	5.0–15.0
	PRMT90		Half saturation constant for nitrate immobilization	$mg\,N\,L^{-1}$	10–20
	PRMT97		Microbial growth rate retardation under anaerobic conditions. $FD_{default}$ = 0.19	–	0.0–1.0
	PRMT98		Nitrifier denitrification coefficient; $ND_{default}$ = 0.0006	–	0.0–0.02
	XKN5		Michaelis-Menten NO_3^- reduction constant	$g\,m^{-3}$	100–500
	XKN3		Michaelis-Menten NO_2^- reduction constant	$g\,m^{-3}$	15–40
	XKN1		Michaelis-Menten N_2O reduction constant	$g\,m^{-3}$	0.01–2.5
	CBVT		Cumulative proportion of the BioVolume of spherical and cylindrical organisms. $CBVT_{default}$ = 0.5	–	0.2–0.8

hydrolysis rate is calculated according to soil organic C, pH, soil temperature, and soil water.

Nitrification is modeled simultaneously with ammonia volatilization in the subroutine NITVOL by combining methods of Reddy et al. (1979) and Godwin et al. (1984), (Williams, 1990). Nitrification follows first-order kinetics and the nitrification rate is affected by soil temperature, water content, and pH. Recently, the nitrification equations were modified to model (a) pH effects on nitrite accumulation and (b) nitrifier denitrification.

We follow Li et al. (2000) to account for nitrifier denitrification (Wrage et al., 2001). Nitrous oxide generated during nitrifier denitrification is calculated as a fraction of nitrification rate (Table 1, PRMT98), as modified by temperature and water-filled porosity functions (Li et al., 2000).

2.7. Gas solubility, phase distribution, and gas transport in soils

Gas solubilities are calculated with formulas from Lide (Lide, 2001) (pages 8–86 to 89. For details see SI Appendix 6.5. Gas Transport). The dimensionless form of Henry's Law Constant (K'$_H$; or air-water partition coefficient) was used to calculate the distribution of these gases between soil air and soil water. K'$_H$ was evaluated using solubility data at a partial pressure of the gas (P_g) of one atmosphere as in SI Appendix 6.5. Gas Transport.

In EPIC-IMWJ mineralization and immobilization of C and N are simulated in a subprogram called NCNMI following the CENTURY model (Izaurralde et al., 2006) with mineralization and immobilization rates varying with fluctuating C/N ratios of microbial biomass following the PHOENIX approach (McGill et al., 1981). Ammonification and N immobilization occur concurrently. All microbial biomass is considered in aggregate – bacterial and fungi are not treated separately. Upper N:C ratios of microbial biomass are set at which ammonification is a maximum and N immobilization ceases; lower N:C ratios of microbial biomass are set at which ammonification ceases and N immobilization is maximum. Ranges of thresholds for N immobilization are tabulated as PRMT 82 and PRMT 83, and for ammonification as PRMT 85 and PRMT 86 in Table 1. At the end of each day, EPIC calculates an amount of C

respired (RSPC, $kg\,ha^{-1}\,d^{-1}$) for each soil layer as controlled by water content and temperature but not [O_2]. To connect CO_2 production with O_2 demand, a new subprogram was developed in EPIC called GASDF3, which uses the one-dimensional gas transport equation to calculate the distribution of [O_2] ($g\,m^{-3}$) at all depths during a 24 h period. Because diffusion in water is about four orders of magnitude slower than in air, diffusion in air is the only mechanism modeled here.

The gas transport equation for any of the three gases modeled (O_2, CO_2, and N_2O) was written as:

$$\frac{\partial(aC_g)}{\partial t} = \frac{\partial^2(D_g^s C_g)}{\partial z^2} + r_g \tag{31}$$

Where, a = volumetric air content ($m^3\,m^{-3}$); C_g = soil gas concentration ($g\,m^{-3}$); r_g = sink (source) term ($g\,m^{-3}$); D_g^s = gas diffusion coefficient in soil ($m^2\,h^{-1}$); t = time (h); and, z = depth (m).

The numerical solutions for the gas transport equation are taken from Press et al. (1993) with modifications to include the volumetric factor. Three solutions are available in the sub model GASDF3 (SI Appendix 6.5. Gas Transport). Users can select the version that most suits their situation. However, the explicit scheme should not be used without adding an explicit check to ensure that the stability criterion is satisfied (Press et al., 1993). We use the Crank-Nicolson solution. The numerical solutions were implemented using the Gaussian elimination procedure followed by back substitution of the tridiagonal matrix (Press et al., 1993; p. 33).

Although the implicit and Crank-Nicholson integration schemes are *stable* for time steps of any size, they are not guaranteed to be *accurate* for large time steps. For most of the calculation, an hourly diffusion time step gives acceptable results, but occasionally, particularly when gas concentrations are changing rapidly (*e.g.,* due to high respiration rates), a one-hour time step is too large. To address this issue, we have introduced an adaptive variable time step into the diffusion solver.

The most obvious indicator of time steps that are too large is diffusive fluxes that are a significant fraction of (or even larger than) the total mass in a grid cell. Accordingly, our adaptive time step

adjusts the time step to limit the maximum fractional change in gas concentration (εC_j^n) over all of the cells in the grid.

$$\max_j \left(C_j^{n+1} - C_j^n \right) < \varepsilon C_j^n$$

If at any point during the integration this condition is violated anywhere in the grid, then the concentrations are rolled back to the beginning of the hour, the time step size is halved, and the integration is restarted. This process continues with the time step being halved at each iteration until the end of an entire hour of integration without encountering a violation. These results are returned to the GASDF3 subroutine for use in the rest of the denitrification model.

Diffusion of a gas in soil is slower than in air because of impediments and tortuosity caused by water-filled pores and soil particles. In addition, diffusion of a dissolving gas is slowed by negligible diffusion rate of the gas contained in the liquid phase. Consequently, the diffusion coefficient of O_2 in soil (D_s) is calculated from the binary diffusion coefficient of O_2 in air (D_a) and a tortuosity factor ξ_g and corrected for dissolution in soil water using K'$_H$ (See SI Appendix 6.5. Gas Transport).

2.8. Gas bubbling

We follow Grant and Pattey (1999) to model the bubbling of N_2O from soil to the atmosphere under anaerobic conditions. Aqueous gas concentrations are limited per the ideal gas law such that dissolved gases are released if the aggregate partial pressures exceed atmospheric pressure. When ebullition occurs, gases are released from solution proportional to the relative concentrations and transferred to the soil surface. Under frozen conditions gases are transferred to the most surficial unfrozen layer while under saturated conditions gases are transported directly to the atmosphere.

3. Methods and data

3.1. Preparing EPIC1704 to run with the IMWJ denitrification submodel

Two types of files are needed to run EPIC: (1) input data files and (2) parameter files (Wang et al., 2012) Input data files are needed to provide to the model: (a) historical daily weather (solar radiation, air temperature, precipitation, relative humidity, wind speed), (b) average monthly weather parameters for simulating daily weather, (c) soil properties (depth, bulk density, field capacity, wilting point, pH, organic C concentration, total N concentration, initial NO_3^- concentration), and (d) management schedules concerning tillage, fertilization, irrigation, and crop operations. Parameter files are needed to specify crop, tillage, fertilizer, and pest characteristics. In addition, other files are needed to specify model options, general parameters, and files to specify weather, site, crop, soil, fertilizer, and pest names to perform single or batch runs (Wang et al., 2012).

Selection of model options, parameter values, and specific input data needed to run EPIC1704 with the IMWJ denitrification submodel are presented in Table 1. The only difference in IDN = 3 or IDN = 4 is the calculation of the water film thickness (DW; Eq. (11); details in SI Appendix 6.3. Calculation of DW). In addition to the original water percolation method in EPIC, two new methods have been implemented recently in EPIC1704 to improve the daily soil water dynamics, particularly in surface soil layers. Setting layer thickness (DZ) will depend on model stability (i.e. model instability will require reduction in DZ; DZ = 0.1 has generally produced stable solutions). Setting the default time interval for solving the gas transport equations (DTG) to 1.0 h generally produces stable solutions of the gas transport equation. Initial gas concentrations

(Table 1; CGO2 = oxygen; CGCO2 = carbon dioxide; CGN2O = nitrous oxide) by soil layer are entered to provide initial conditions for the gas transport equation. For O_2, the values should be entered in decreasing order by depth, while the opposite should be done for the two trace gases. Boundary gas concentrations (air and bottom of soil profile) are hard coded.

The N mineralization-immobilization submodel in EPIC1704 (NCNMI) follows the approach used in PHOENIX (McGill et al., 1981). Upper and lower N:C ratios of microbial biomass were noted above (Table 1; PRMT 82, 83, 85, 86). Table 1 also includes ranges of values for half saturation constants for ammonium immobilization (PRMT88), nitrite immobilization (PRMT89), and nitrate immobilization (PRMT90) together with the specific base rate of ammonification (PRMT 84) and the maximum rate of N uptake during immobilization (PRMT87). Finally, the Michaelis-Menten constant values XKN5, XKN3, and XKN1 can be either selected from the range provided in Table 1, from literature values (see SI Appendix 6.6. Range and means of Michaelis constant (Km) values reported in the literature), or determined via model optimization (see below Section 3.3. Description of the simulation experiment).

3.2. Description of experimental data used to test the IMWJ denitrification model in EPIC

We used results from a 2-year field experiment conducted in 2007 and 2008 at five locations (four on-farm, one at Michigan St. Univ. W.K. Kellogg Biological Station [KBS]) in Michigan (Hoben et al., 2011) to test the non-linear response of N_2O fluxes as a function of linearly increasing N fertilizer rates. Of the five locations, only three had two years of data, of which the KBS site (42°41N, 85°37W) offered the best weather and soil data to parameterize input files and perform simulations due to extensive experimentation and excellent records. Thus, we selected the KBS site to test the IMWJ model in EPIC.

An N-rate experiment with maize (*Zea mays* L.) was conducted in 2007 on a Kalamazoo loam (fine-loamy, mixed, mesic Typic Hapludalf) and repeated in 2008 on an adjacent field on the same soil series. Each crop of maize followed a crop of soybean (*Glycine max* L. Merr.). These fields had been under grain production following management practices common to the region before initiation of the experiment. Winter wheat (*Triticum aestivum* L.) was grown as a cover crop after soybean harvest and was terminated with herbicides prior to maize planting. The experimental design was a randomized complete block design with six rates of N (0, 45, 90, 135, 180, and 225 kg N ha^{-1}) and four replications. Fertilizer urea was broadcast and incorporated to a depth of 10 cm two days before maize planting in early May. Further experimental details can be found in Hoben et al. (2011).

Static chambers were used to obtain gas samples for determination of N_2O concentration and subsequent calculation of N_2O fluxes. Gas samples for N_2O flux determination were obtained once before planting, every other day after fertilization for 15 days, then weekly for 30 days, and finally every 10–14 days after 45 days until crop harvest. For details on gas sampling, concentration measurements, and flux calculations see Hoben et al. (2011)

3.3. Description of the simulation experiment

Information about file structure and content needed to perform single to multiple EPIC runs with a Fortran-based executable can be obtained from http://epicapex.tamu.edu/manuals-and-publications/

To prepare the weather data for the simulations, daily records of precipitation, air temperature, solar radiation, wind direction and speed, and relative humidity were retrieved from the KBS Long Term Ecological Research site (http://lter.kbs.msu.edu/datatables/

Table 2
Model evaluation statistics.

Year	Variable	R^2	NSE	RMSE	Bias
2007	Grain yield	0.00604	−4.67	0.270	−7.8
2007	Cumulative N_2O flux	0.878	−1.30	0.670	77.7
2007	Daily N_2O flux	0.918	0.619	0.00458	28.5
2007	Soil inorganic N (0–10 cm)	0.991	−2.16	33.331531	61.4
2008	Grain yield	0.0333	−15.4	1.68	53.5
2008	Cumulative N_2O flux	0.780	0.692	0.387	15.7
2008	Daily N_2O flux	0.778	0.511	0.00396	−3.3
2008	Soil inorganic N (0–10 cm)	0.981	0.979	4.12	1.6

75) for the period 1988–2008. The soil input data were obtained based on the characteristics of the Kalamazoo loam series (SSURGO, Soil Survey Geographic Database; http://www.nrcs.usda.gov/wps/portal/nrcs/detail/soils/survey/?cid=nrcs142p2_053627) for horizon depth, water limits, saturated conductivity, texture, and soil organic carbon. The soil properties were modified with available site-specific soil data (texture, bulk density, soil organic carbon, and water limits).

Simulations were initiated with a 15 year spin-up run with a maize-soybean rotation to represent historical land management followed by the one year considered in the Hoben et al. (2011) experiment as described above. The final year of the spin-up simulation included a soybean crop followed by a winter wheat cover crop terminated in spring of the measurement year. Finally, the maize crop during the measurement year was fertilized with the various N rates as above. Initial conditions for soil organic carbon and cation exchange capacity were adjusted per data reported in Hoben et al. (2011) and data from nearby experiments on the same soil series. Finally, we used measured N_2O fluxes and surface soil inorganic N from 2007 to calibrate the model and from 2008 to validate the model as described in the following Section. Model optimization for the 2007 calibration dataset yielded the following values for the Michaelis-Menten constant values: XKN5 = 36.9, XKN3 = 21.0, and XKN1 = 9.9.

3.4. Evaluation of model performance

An initial group of parameters were identified with potential for impacting the simulated N cycling, and Morris's elementary screening method (Morris, 1991) was implemented to assess parameter sensitivity and reduce the number of parameters to consider in the calibration. Parameters were assumed to be uniformly distributed within ranges specified from literature values, model documentation or expert knowledge (see SI Appendix 6.7. Parameters and ranges considered for Morris Method sensitivity analysis and Appendix 6.8. Relative importance metric of parameters per sensitivity of the NSE of the simulated versus measured daily N_2O flux). The selected group of parameters (PRMT97, PRMT98, XKN1, XKN3, XKN5, FC1, FC2, FC3, BD1, BD2, and BD3) were estimated using the NSGA-II multi-objective genetic parameter estimation algorithm (Deb et al., 2002). The average Nash-Sutcliffe coefficient of efficiency (NSE) was calculated for the soil inorganic N in the upper 10 cm, which was measured on 3–4 dates within roughly 30 days following fertilizer application and averaged, across fertilizer treatments as well as the daily N_2O flux across treatments. The average of these two NSE values was used as the objective function to maximize. Additionally, correlation coefficient (R^2), root-mean-square-error (RMSE), and percent bias (bias) were calculated to characterize model fit. These statistics were calculated using the same procedure as described above for daily N_2O flux and inorganic soil N. For cumulative N_2O flux, the total seasonal fluxes across treatments were considered while for yield the harvested

yields were considered across treatments. All sensitivity and calibration procedures were conducted in R version 3.2.1 (R Core Team, 2014). Soil parameters were optimized and held constant during the multi-year simulations. Model parameters were optimized during the calibration year (2007) and utilized during the validation year (2008). Model performance for the 2007 and 2008 years was assessed per NSE, coefficient of determination (R^2), root-mean-square error (RMSE) and percent bias (bias).

4. Results and discussion

4.1. Growing season conditions and maize yields at KBS during 2007 and 2008

As documented by Hoben et al. (2011), maize experienced periods of drought during both growing seasons. In 2007, annual precipitation was equal to the 30-yr normal (885 mm) and growing-season precipitation (May–October) was 5% below the normal (529 mm). However, monthly precipitation was below normal during May (−21%), June (−34%), July (−66%), and September (−36%). In 2008, annual precipitation exceeded the normal by 20% and growing-season precipitation was 19% above the normal. Again, monthly precipitation was significantly below normal during May (−39%) and August (−72%). Not surprisingly, reported mean maize (dry) yields were low in both years (3.14 ± 0.05 Mg ha^{-1} in 2007 and 3.05 ± 0.19 Mg ha^{-1} in 2008). In 2007, maize yields did not respond to fertilizer N application while in 2008 there was a polynomial yield response to N application, which peaked at the rate of 90 kg N ha^{-1}. However, simulated yields did not show any response to fertilizer N application in either year. In 2007, the mean simulated yield was 8% lower than the observed (2.89 ± 0.00 Mg ha^{-1}) while in 2008 it was 55% higher than the observed (4.72 ± 0.08 Mg ha^{-1}) (Table 2). In both years, the yield difference between observed and simulated yields was statistically significant at p < 0.01. In both years, there was a lack of correlation between observed and simulated yields (R^2_{2007} = 0.03NS; R^2_{2008} = 0.01NS). In both years as well, differences in simulated yields were largely explained by water stress. In 2007, EPIC simulated 70 days of water stress days during the growing season while in 2008 the number of simulated stress days was 59. Apparently, the effect of simulated water stress on yield in 2008 was less impactful than in 2007 leading to the yield differences between simulated values and reported observations during the second year (Hoben et al., 2011).

4.2. Observed and simulated (A) daily and (B) cumulative N_2O fluxes at KBS for six N rates in 2007 and 2008

As described above, in each year, for each N rate treatment, there were 26–30 observations of N_2O flux available for comparison against simulated N_2O fluxes. In contrast, the simulated daily N_2O fluxes were available for the entire growing season (~153 days)
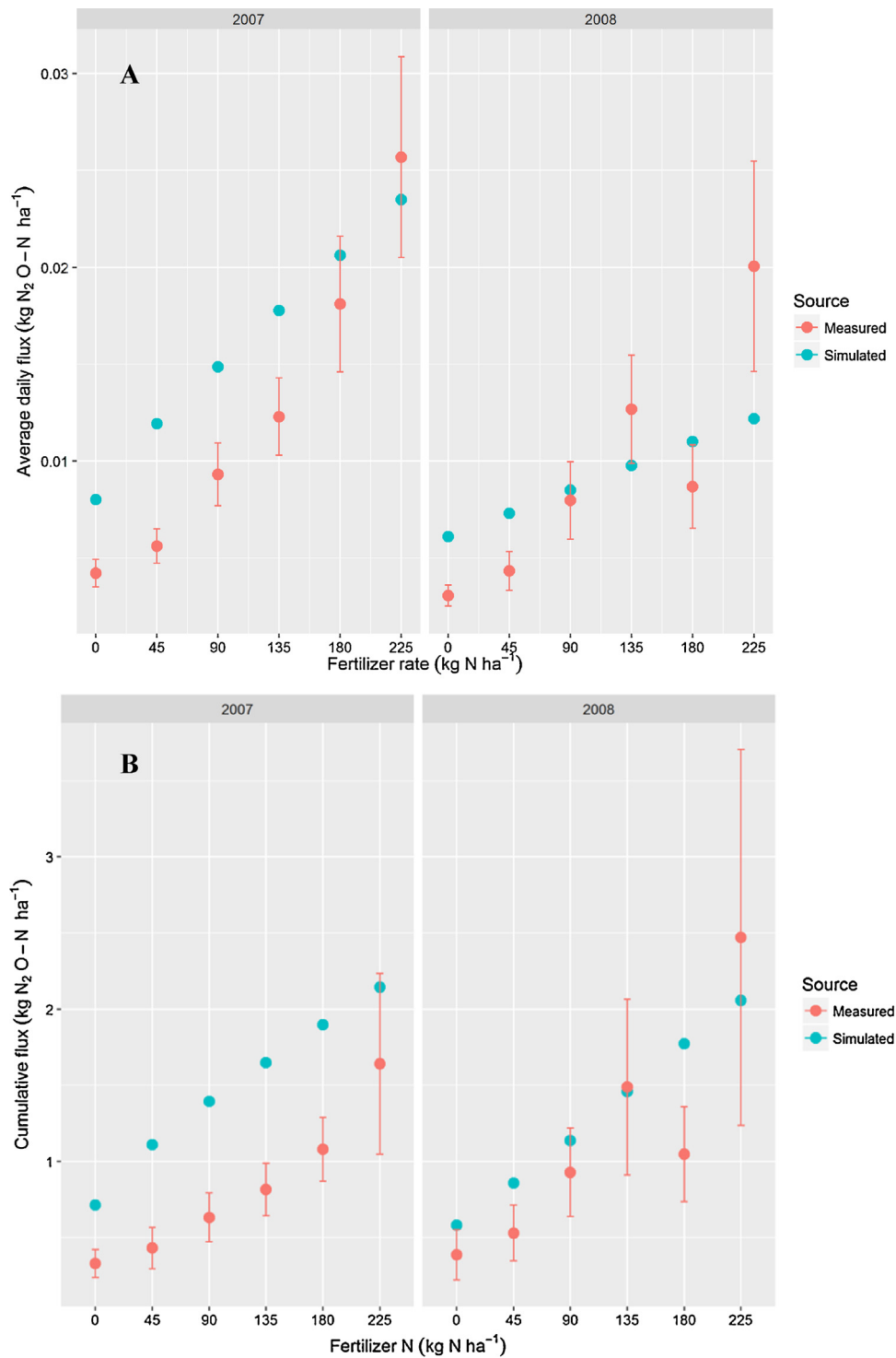
Fig. 2. Observed and simulated (A) daily and (B) cumulative N$_2$O fluxes at KBS for six N rates in 2007 and 2008.

where each daily flux resulted from the sum of 24 hourly fluxes. Thus, comparisons of simulated vs. measured daily fluxes were restricted to days with available observations while comparisons of seasonal N$_2$O-fluxes were made between cumulative fluxes resulting from summation of daily simulated values and fluxes obtained from linear interpolation of observed fluxes.

Fig. 2A displays observed and simulated average daily N$_2$O fluxes as affected by N rates during the calibration (2007) and the validation (2008) years. Similarly, Fig. 2B shows observed and simulated cumulative N$_2$O fluxes as influenced by N rates during

the calibration and validation years. In both comparisons, there was a clear correlation between average observed and simulated values ($R^2_{2007} = 0.918$, $p < 0.003$; $R^2_{2008} = 0.778$, $p < 0.02$). A more detailed comparison revealed statistically significant correlations (Fig. 3) between observed and simulated daily N$_2$O fluxes arranged by N rate and year. Occasional flux under-predictions at N rates >135 kg N ha^{-1} occurred in both years.

Observed average daily N$_2$O fluxes increased exponentially with N rate in both years (Fig. 2A) (Hoben et al., 2011). In 2007, simulated fluxes approximated the observed fluxes in magnitude but the
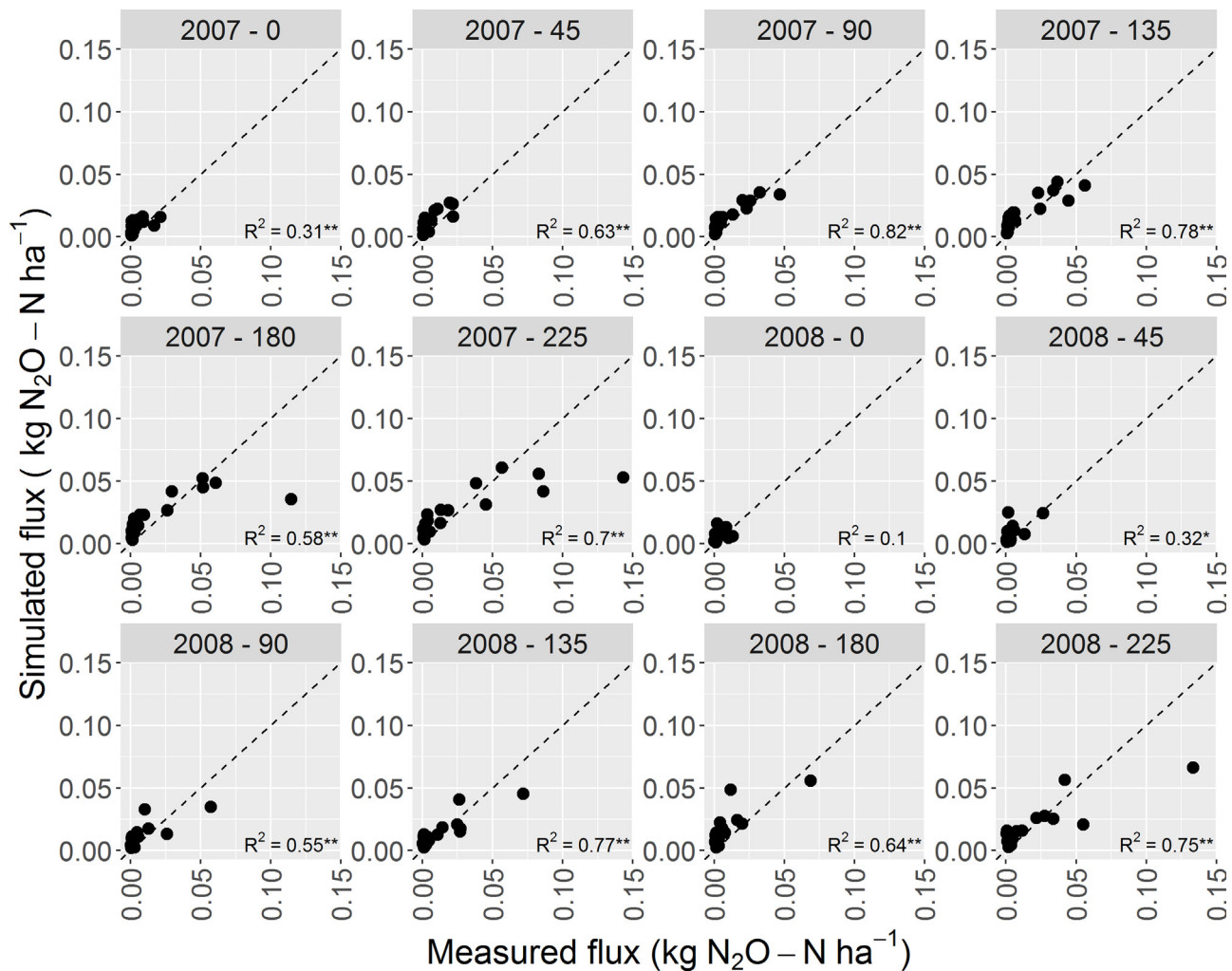
Fig. 3. Observed versus simulated N_2O fluxes at KBS for six N rates during 2007 and 2008. R-square values and their significance arranged by year and N rate are presented in Fig. 3. One asterisk represents statistical significance at $p < 0.05$ while two asterisks indicate significance at $p < 0.01$.

relationship was linear instead of exponential. In 2008, the slope of the linear increase of the simulated N_2O fluxes was less pronounced than the observed fluxes. In contrast, observed cumulative N_2O fluxes showed an exponential behavior only in 2007. While an exponential fit was also used to describe the 2008 data, the unexpectedly low cumulative N_2O flux observed for the 180 N rate opens the possibility that, after removal of the data point, a linear fit would have been an equal or better model (adjusted $R^2 = 0.98^{**}$) relative to the exponential fit (adjusted $R^2 = 0.97^{**}$). Simulated cumulative fluxes followed the increasing trends of the observations but there was a closer match between observed and simulated fluxes in 2008 than in 2007.

Three reasons are offered to help explain the simulated linear instead of exponential increase in average daily and cumulative N_2O fluxes in response to six rates of N application. First, there was a rather modest observed and simulated increase in maize biomass, which limited the increase in root respiration and thus constrained the demand of electron acceptors. Second, microbial respiration increased curvilinearly in response to N additions reaching a ~10% increase with the highest rate ($y_{2007} = -2E-6x^2 + 8E-4x + 1.01$, $R^2 = 0.86^{**}$; $y_{2008} = -1E-6x^2 + 8E-4x + 1.0$, 0.98^{**}). And last, both observed and simulated soil NO_3^- were highly correlated (Table 2) and both increased linearly in response to N fertilization (R-squares ≥ 0.98 for observed and simulated values; see Table 2 in Hoben et al. (2011) for observed values). However, while the

observed relationship between mineral N and N_2O flux was exponential ($y_{2007} = 1.23e^{0.03x}$, $R^2 = 0.99^{**}$; $y_{2008} = 2.32e^{0.02x}$, $R^2 = 0.98^{**}$) the simulated relationship between mineral N and N_2O flux was linear ($y_{2007} = 1.43E-2x+0.97$, $R^2 = 0.98^{**}$; $y_{2008} = 2.17E-2x + 0.76$, 0.99^{**}). Whether linear or exponential, the results are consistent with experimental data showing greater potential for denitrifiers to produce more N_2O relative to N_2 at higher levels of N input/NO_3^- availability (Senbayram et al., 2012). The change in product $N_2O/(N_2O+N_2)$ ratios as a function of NO_3^- availability could not be tested here due to lack of N_2 data and thus remains a topic of research.

Nonlinear increases of N_2O fluxes in response to linear rates of N application up to 300 kg N ha^{-1} have been simulated also with the *ecosys* model after previous parameterization using agronomic and eddy covariance data from fertilized fields near Ottawa, Canada (Grant et al., 2006). The reported simulated exponential rise, however, was tenuous enough allowing for the possibility to describe the relationship between N_2O flux and N rate with a linear fit. Global *meta*-analysis (Bouwman et al., 2002; Kim et al., 2013; Shcherbak et al., 2014) and modeling (Philibert et al., 2012, 2014) strongly suggests a nonlinear rise of N_2O fluxes in response to N additions, especially when crop needs are exceeded. In our study, applied N rates exceeded crop N needs as seen in the flat yield response caused by droughty conditions. While simulated increases in microbial respiration, CO_2 flux, and soil NO_3^- help
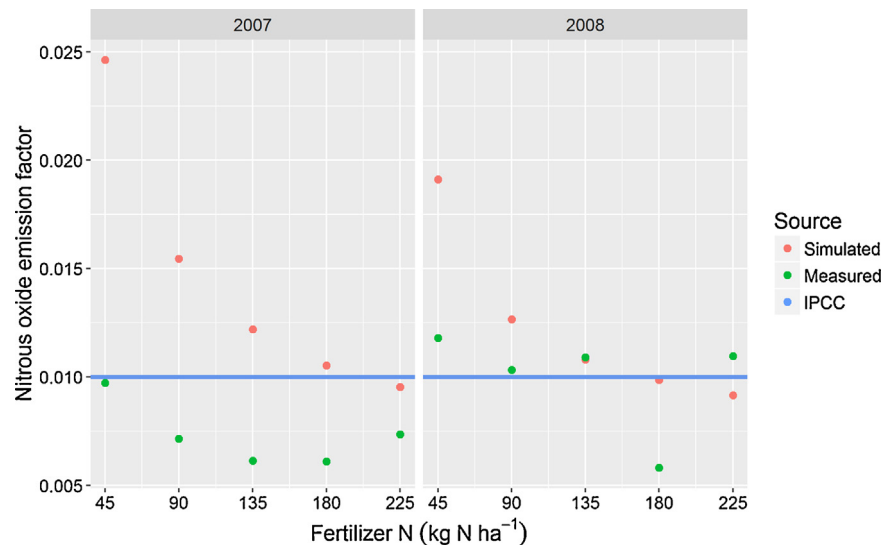
Fig. 4. Observed, simulated, and IPCC Nitrous Oxide Emission Factors for the KBS N rate (kg ha^{-1}) experiment.

explain the simulated linear increases in N$_2$O flux, there remains a clear need to improve/develop modeling mechanisms in EPIC to capture the exponential behavior of observed N$_2$O flux in response to N rate reported by Hoben et al. and other experiments (Hoben et al., 2011; Shcherbak et al., 2014).

Understanding the response of N$_2$O emissions to fertilizer N application has policy and practical implications. Regarding the policy implication, the observed and simulated results presented here can be used to evaluate the IPCC Tier 1 emission factor (1% of N inputs converted to N$_2$O) (Fig. 4). Simulated responses decreased exponentially with N rate in both years, were higher than the 1% factor at lower N rates, and approached the 1% factor at higher rate. The observed responses also generally showed exponential decreased with N rate. The observed factor was lower than 1% in 2007 while it surpassed slightly the IPCC factor in 2008.

Concerning a practical application, exponential models—based in part on data from Hoben et al. (2011)—form the basis of N$_2$O mitigation protocols at three of the major international carbon standard organizations (Verified Carbon Standard (VCS). http://www.v-c-s.org/; American Carbon Registry (ACR). http://americancarbonre-gistry.org/, and Climate Action Reserve (CAR). http://www.climateactionre-serve.org/; Millar et al., 2010, 2012, 2013). These protocols allow farmers to convert their N$_2$O emissions reductions to equivalent units of carbon dioxide (CO$_{2e}$) that can be traded as carbon credits on environmental markets to generate income.

There are pros and cons to using emissions factors (Tier 1) and more complex process-based models (Tier 3) in this context. In both cases, the use of empirical data to validate model performance and quantify uncertainty is essential. For example, Tier 1 models are more straightforward to use, less costly to operate, and often offer similar or improved performance in estimating N$_2$O emissions and mitigation. However, they are inherently limited in their application if multiple management practices are being investigated concurrently and likely less reliable in estimating fluxes over shorter periods. When options are available, model selection should be made based on intended use (Hillier et al., 2016).

4.3. Analysis of stocks and fluxes of selected variables related to microbial denitrification simulated with EPIC

Nitrous oxide fluxes at the soil surface arise in response to complex physical and biological interactions that occur across time and space. Fig. 5 illustrates the spatiotemporal dynamics of liquid and gaseous ions and molecules simulated by EPIC as they interact in the soil and, in the case of CO$_2$, N$_2$O, and N$_2$ evolve into the atmosphere. The figure shows precipitation, N$_2$O fluxes at the soil surface, soil water, N$_2$O in liquid and gas phases, NO$_3^-$, and O$_2$ in gas phase. The first column of plots in the illustration corresponds to the 0 kg N ha^{-1} fertilization rate while the second column corresponds to the 135 kg N ha^{-1} rate.

The first noticeable event is the N$_2$O flux simulated (but lacking observations) in early April in both unfertilized and fertilized plots. During that period, soil water content was relatively high in the top half of the soil profile. Concurrently, (a) O$_2$ concentration in the gas phase was starting to increase in the top 50-cm soil depth but remained low throughout the rest of the soil profile, (b) nitrate levels were low throughout the soil profile, and (c) there was simulated N$_2$O accumulation at depth. All these events seem to coincide with the release of N$_2$O to the atmosphere via the gas phase and likely aided by bubbling events.

The second event of N$_2$O release started soon after fertilization and maize planting in early May. Observed and simulated N$_2$O increased rapidly during this period, peaked in mid-June, coinciding with a rainy period, and then declined (rapidly at first until the end of June, gradually afterwards) toward the end of July. Nitrate levels in the top soil layers were elevated during this period, especially in June. This seems to support the hypothesis that the peak release of N$_2$O during the rainy period in June corresponded to high NO$_3^-$ levels in surface soils, periodic high levels of soil water content, and restricted entrance of O$_2$ into the soil. A significant rainy period toward the end of September seemed to have caused small observed and simulated N$_2$O releases. We surmise this was due to low levels of nitrates in the soil profile.

5. Summary and conclusions

Here we have documented IMWJ, a novel microbial denitrification model implemented in the terrestrial ecosystem model EPIC. The IMWJ model is based on fundamental principles of biology, chemistry, and physics. Provided the EPIC model is calibrated well for plant productivity, water, carbon, and nutrient cycling, the IMWJ submodel requires further calibration of only a few parameters, especially the affinity coefficients used in the Michaelis-Menten competitive inhibition equations.
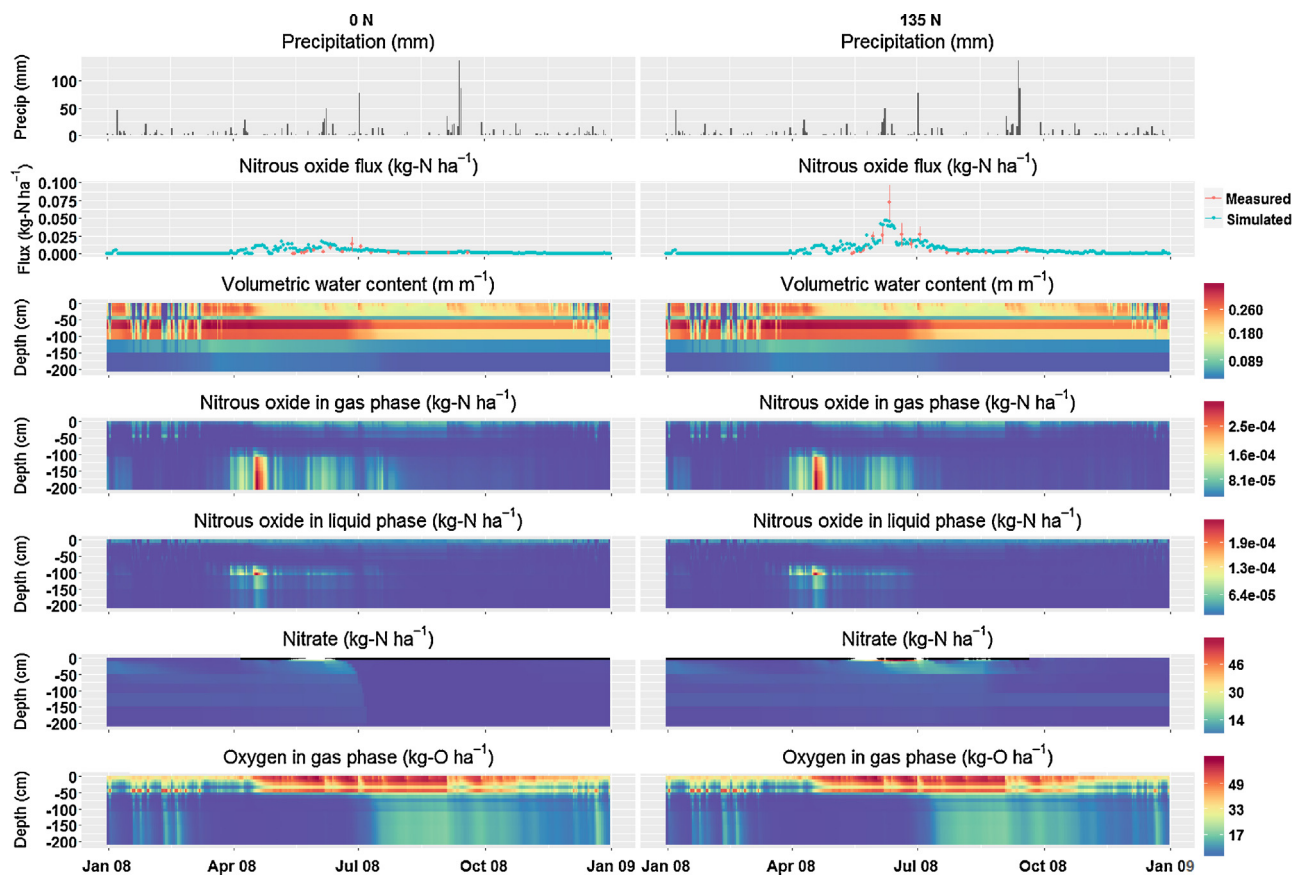
Fig. 5. One and two dimensional graphs showing stocks and fluxes of variables related to microbial denitrification and N$_2$O fluxes in a Typic Hapludalf cropped to maize during 2008 at the Michigan State University Kellogg Biological Station.

We have tested the IMWJ model against data from an experiment designed to test the generation of N$_2$O fluxes after applying six rates of fertilizer N to maize plots. The modeled data tracked the measured increase of the daily and seasonal N$_2$O fluxes. However, the shape of the 3-fold increase in N$_2$O fluxes was simulated as linear instead of the measured exponential response. It should be noted that both the measured and modeled N$_2$O-flux responses arose upon the sudden change in fertilization regime (i.e., onetime fertilization following a common management history).

We conclude that EPIC—implemented with the IMWJ option—could approximate acceptably well the timing and magnitude of N$_2$O fluxes plus several environmental variables such as crop yields (and the lack of yield response to nitrogen application due to droughty conditions), water stress, surficial soil-water dynamics, and nitrate mass in surface layers after fertilization. However, the model did not capture the observed exponential trend in N$_2$O fluxes (Hoben et al., 2011). Detailed experiments comparing simulated and measured N$_2$O fluxes under variable N rates as was done here are scarce in the literature. Further model testing of EPIC+IMWJ, alone or in ensemble with other models, using data from comprehensive experiments will be essential to discover areas of model improvement and increase the accuracy of N$_2$O predictions under a wide range of environmental conditions.

Acknowledgements

Appendix A. Supplementary data

Supplementary data associated with this article can be found, in the online version, at http://dx.doi.org/10.1016/j.ecolmodel.2017.06.007.

References

Bouwman, A.F., Boumans, L.J.M., Batjes, N.H., 2002. Modeling global annual N2O and NO emissions from fertilized fields. Glob. Biogeochem. Cycles 16, 1080, http://dx.doi.org/10.1029/2001GB001812.

Campbell, G.S., 1985. Soil Physics with Basic: Transport Models for Soil-Plant Systems. Elsevier, Amsterdam, The Netherlands.

Chen, D., Li, Y., Grace, P., Mosier, A.R., 2008. N2O emissions from agricultural lands: a synthesis of simulation approaches. Plant Soil 309, 169–189, http://dx.doi.org/10.1007/s11104-008-9634-0.

Ciais, P., Sabine, C., Bala, G., Bopp, L., Brovkin, V., Canadell, J., Chhabra, A., DeFries, R., Galloway, J., Heimann, M., et al., 2014. Carbon and other biogeochemical cycles, in: climate change 2013: the physical science basis. In: Contribution of

Working Group I to the Fifth Assessment Report of the Intergovernmental Panel on Climate Change. Cambridge University Press, pp. 465–570.

Conrad, R., 1996. Soil microorganisms as controllers of atmospheric trace gases (H-2, CO, CH 4, OCS, N2O, and NO). Microbiol. Rev. 60 (609-+).

Crank, J., Nicolson, P., 1996. A practical method for numerical evaluation of solutions of partial differential equations of the heat-conduction type. Adv. Comput. Math. 6, 207–226.

Crutzen, P., 1970. Influence of nitrogen oxides on atmospheric ozone content. Q. J. R. Meteorol. Soc. 96, 320-, http://dx.doi.org/10.1002/qj.49709640815.

Davidson, E.A., 2009. The contribution of manure and fertilizer nitrogen to atmospheric nitrous oxide since 1860. Nat. Geosci. 2, 659–662, http://dx.doi.org/10.1038/NGEO608.

De Klein, C., Novoa, R.S.A., Ogle, S., Smith, K.A., Rochette, P., Wirth, T.C., McConkey, B.G., Mosier, A., Rypdal, K., n.d. 11: N2O emissions from managed soils, and CO2 emissions from lime and urea application, in: In 2006 IPCC Guidelines for National Greenhouse Gas Inventories, Vol. 4: Agriculture, Forestry and Other Land Use (AFOLU). p. 677 pp.

Deb, K., Pratap, A., Agarwal, S., Meyarivan, T., 2002. A fast and elitist multiobjective genetic algorithm: NSGA-II. Ieee Trans. Evol. Comput. 6, 182–197, http://dx.doi.org/10.1109/4235.996017.

Del Grosso, S.J., Parton, W.J., Mosier, A.R., Ojima, D.S., Kulmala, A.E., Phongpan, S., 2000. General model for N2O and N-2 gas emissions from soils due to denitrification. Glob. Biogeochem. Cycles 14, 1045–1060.

Del Grosso, S.J., Parton, W.J., Mosier, A.R., Walsh, M.K., Ojima, D.S., Thornton, P.E., 2006. DAYCENT national-scale simulations of nitrous oxide emissions from cropped soils in the United States. J. Environ. Qual. 35, 1451–1460, http://dx.doi.org/10.2134/jeq2005.0160.

Frolking, S.E., Mosier, A.R., Ojima, D.S., Li, C., Parton, W.J., Potter, C.S., Priesack, E., Stenger, R., Haberbosch, C., Dorsch, P., Flessa, H., Smith, K.A., 1998. Comparison of N(2)O emissions from soils at three temperate agricultural sites: simulations of year-round measurements by four models. Nutr. Cycl. Agroecosyst. 52, 77–105, http://dx.doi.org/10.1023/A:1009780109748.

Godwin, D.C., Jones, C.A., 1991. Nitrogen dynamics in soil-plant systems. In: Modeling Plant and Soil Systems, Agronomy Monograph. ASA-CSSA-SSSA, Segoe Road, Madison, Wisconsin 53711, USA, pp. 287–321.

Grant, R.F., Pattey, E., 1999. Mathematical modeling of nitrous oxide emissions from an agricultural field during spring thaw. Glob. Biogeochem. Cycles 13, 679–694, http://dx.doi.org/10.1029/1998GB900018.

Grant, R., Nyborg, M., Laidlaw, J., 1993a. Evolution of nitrous-oxide from soil. 1. Model Development. Soil Sci. 156, 259–265, http://dx.doi.org/10.1097/00010694-199310000-00006.

Grant, R., Nyborg, M., Laidlaw, J., 1993b. Evolution of nitrous-oxide from soil. 2. Experimental results and model testing. Soil Sci. 156, 266–277, http://dx.doi.org/10.1097/00010694-199310000-00007.

Grant, R.F., Pattey, E., Goddard, T.W., Kryzanowski, L.M., Puurveen, H., 2006. Modeling the effects of fertilizer application rate on nitrous oxide emissions. Soil Sci. Soc. Am. J. 70, 235–248, http://dx.doi.org/10.2136/sssaj2005.0104.

Hillier, J., Abdalla, M., Bellarby, J., Albanito, F., Datta, A., Dondini, M., Fitton, N., Hallett, P., Hastings, A., Jones, E., Kuhnert, M., Nayak, D., Pogson, M., Richards, M., Smith, J., Vetter, S., Yeluripati, J., Smith, P., 2016. Mathematical modeling of greenhouse gas emissions from agriculture for different end users. In: DelGrosso, S.J., Ahuja, L.R., Parton, W.J. (Eds.), Synthesis and Modeling of Greenhouse Gas Emissions and Carbon Storage in Agricultural and Forest Systems to Guide Mitigation and Adaptation. , pp. 197–227.

Hoben, J.P., Gehl, R.J., Millar, N., Grace, P.R., Robertson, G.P., 2011. Nonlinear nitrous oxide (N2O) response to nitrogen fertilizer in on-farm corn crops of the US Midwest. Glob. Change Biol. 17, 1140–1152, http://dx.doi.org/10.1111/j.1365-2486.2010.02349.x.

Izaurralde, R.C., Williams, J.R., McGill, W.B., Rosenberg, N.J., Jakas, M.C.Q., 2006. Simulating soil C dynamics with EPIC: Model description and testing against long-term data. Ecol. Model. 192, 362–384, http://dx.doi.org/10.1016/j.ecolmodel.2005.07.010.

Khalil, M. a. K., Rasmussen, R.A., Shearer, M.J., 2002. Atmospheric nitrous oxide: patterns of global change during recent decades and centuries. Chemosphere 47, 807–821, http://dx.doi.org/10.1016/S0045-6535(01)00297-1.

Kim, D.-G., Hernandez-Ramirez, G., Giltrap, D., 2013. Linear and nonlinear dependency of direct nitrous oxide emissions on fertilizer nitrogen input: a meta-analysis. Agric. Ecosyst. Environ. 168, 53–65, http://dx.doi.org/10.1016/j.agee.2012.02.021.

Kool, D.M., Dolfing, J., Wrage, N., Van Groenigen, J.W., 2011. Nitrifier denitrification as a distinct and significant source of nitrous oxide from soil. Soil Biol. Biochem. 43, 174–178, http://dx.doi.org/10.1016/j.soilbio.2010.09.030.

Li, C., Frolking, S., Frolking, T., 1992. A model of nitrous-oxide evolution from soil driven by rainfall events. 2. Model applications. J. Geophys. Res.-Atmos. 97, 9777–9783.

Li, C.S., Narayanan, V., Harriss, R.C., 1996. Model estimates of nitrous oxide emissions from agricultural lands in the United States. Glob. Biogeochem. Cycles 10, 297–306, http://dx.doi.org/10.1029/96GB00470.

Li, C.S., Aber, J., Stange, F., Butterbach-Bahl, K., Papen, H., 2000. A process-oriented model of N2O and NO emissions from forest soils: 1. Model development. J. Geophys. Res.-Atmos. 105, 4369–4384, http://dx.doi.org/10.1029/1999JD900949.

Li, Y., Chen, D.L., Zhang, Y.M., Edis, R., Ding, H., 2005. Comparison of three modeling approaches for simulating denitrification and nitrous oxide emissions from loam-textured arable soils. Glob. Biogeochem. Cycles 19, B3002, http://dx.doi.org/10.1029/2004GB002392.

Lide, D.R., 2001. CRC Handbook of Chemistry and Physics, 82nd ed. CRC Press, Boca Raton, FL.

McGill, W.B., Hunt, H.W., Woodmansee, R.G., Reuss, J.O., 1981. Phoenix a model of the dynamics of carbon and nitrogen in grassland soils. In: Clark, F.E., Rosswall, T. (Eds.), Ecological Bulletins Nfr (Naturvetenskapliga Forskningsradet) No. 33. Terrestrial Nitrogen Cycles: Processes, Ecosystem Strategies and Management Impacts; Proceedings of an International Workshop. Osterfarnebo, Sweden, Sept. 16–22, 1979. 714p. Swedish Natural Science Research Council: Stockholm, Sweden. Illus, pp. 49–116.

Millar, N., Robertson, G.P., Grace, P.R., Gehl, R.J., Hoben, J.P., 2010. Nitrogen fertilizer management for nitrous oxide (N2O) mitigation in intensive corn (Maize) production: an emissions reduction protocol for US Midwest agriculture. Mitig. Adapt. Strateg. Glob. Change 15, 185–204, http://dx.doi.org/10.1007/s11027-010-9212-7.

Millar, N., Robertson, G.P., Diamant, A., Gehl, R.J., Grace, P.R., Hoben, J.P., 2012. Methodology for Quantifying Nitrous Oxide (N2O) Emissions Reductions by Reducing Nitrogen Fertilizer Use on Agricultural Crops American Carbon Registry. Winrock International, Little Rock, AK.

Millar, N., Robertson, G.P., Diamant, A., Gehl, R.J., Grace, P.R., Hoben, J.P., 2013. Quantifying N2O Emissions Reductions in US Agricultural Crops Through N Fertilizer Rate Reduction. Winrock International, Little Rock, AK.

Millington, R., Quirk, J., 1961. Permeability of porous solids. Trans. Faraday Soc. 57, 1200, http://dx.doi.org/10.1039/tf9615701200.

Morris, M., 1991. Factorial sampling plans for preliminary computational experiments. Technometrics 33, 161–174, http://dx.doi.org/10.2307/1269043.

Mosier, A.R., Duxbury, J.M., Freney, J.R., Heinemeyer, O., Minami, K., 1996. Nitrous oxide emissions from agricultural fields: assessment, measurement and mitigation. Plant Soil 181, 95–108, http://dx.doi.org/10.1007/BF00011296.

Nol, L., Heuvelink, G.B.M., Veldkamp, A., de Vries, W., Kros, J., 2010. Uncertainty propagation analysis of an N2O emission model at the plot and landscape scale. Geoderma 159, 9–23, http://dx.doi.org/10.1016/j.geoderma.2010.06.009.

Parton, W.J., Mosier, A.R., Ojima, D.S., Valentine, D.W., Schimel, D.S., Weier, K., Kulmala, A.E., 1996. Generalized model for N-2 and N2O production from nitrification and denitrification. Glob. Biogeochem. Cycles 10, 401–412, http://dx.doi.org/10.1029/96GB01455.

Philibert, A., Loyce, C., Makowski, D., 2012. Quantifying uncertainties in N2O emission due to N fertilizer application in cultivated areas. PLoS One 7, e50950, http://dx.doi.org/10.1371/journal.pone.0050950.

Philibert, A., Loyce, C., Makowski, D., 2014. Predicting nitrous oxide emissions with a random-effects model. Environ. Model. Softw. 61, 12–18, http://dx.doi.org/10.1016/j.envsoft.2014.07.002.

Press, W.H., Teukolsky, S.A., Vetterling, W.T., Flannery, B.P., 1993. Numerical Recipes in FORTRAN; The Art of Scientific Computing, 2nd ed. Cambridge University Press, New York, NY.

R Core Team, 2014. R: a Language and Environment for Statistical Computing.

Robertson, G.P., Groffman, P.M., 2015. Nitrogen Transformations, In: Soil Microbiology, Ecology and Biochemistry. Elsevier, pp. 421–446, http://dx.doi.org/10.1016/B978-0-12-415955-6.00014-1.

Robertson, G., Tiedje, J., 1987. Nitrous-oxide sources in aerobic soils – nitrification, denitrification and other biological processes. Soil Biol. Biochem. 19, 187–193, http://dx.doi.org/10.1016/0038-0717(87)90080-0.

Robertson, G.P., Paul, E.A., Harwood, R.R., 2000. Greenhouse gases in intensive agriculture: contributions of individual gases to the radiative forcing of the atmosphere. Science 289, 1922–1925, http://dx.doi.org/10.1126/science.289.5486.1922.

Robertson, G.P., Bruulsema, T.W., Gehl, R.J., Kanter, D., Mauzerall, D.L., Rotz, C.A., Williams, C.O., 2013. Nitrogen–climate interactions in US agriculture. Biogeochemistry 114, 41–70, http://dx.doi.org/10.1007/s10533-012-9802-4.

Roco, C.A., Bergaust, L.L., Shapleigh, J.P., Yavitt, J.B., 2016. Reduction of nitrate to nitrite by microbes under oxic conditions. Soil Biol. Biochem. 100, 1–8, http://dx.doi.org/10.1016/j.soilbio.2016.05.008.

Rodhe, H., 1990. A comparison of the contribution of various gases to the greenhouse-Effect. Science 248, 1217–1219, http://dx.doi.org/10.1126/science.248.4960.1217.

Saggar, S., Jha, N., Deslippe, J., Bolan, N.S., Luo, J., Giltrap, D.L., Kim, D.G., Zaman, M., Tillman, R.W., 2013a. Denitrification and N2O:N2 production in temperate grasslands Processes, measurements, modelling and mitigating negative impacts. Sci. Total Environ. 465, 173–195.

Saggar, S., Jha, N., Deslippe, J., Bolan, N.S., Luo, J., Giltrap, D.L., Kim, D.-G., Zaman, M., Tillman, R.W., 2013b. Denitrification and N2O:N-2 production in temperate grasslands: processes, measurements, modelling and mitigating negative impacts. Sci. Total Environ. 465, 173–195, http://dx.doi.org/10.1016/j.scitotenv.2012.11.050.

Scott, D.H., 2000. Soil Physics: Agricultural and Environmental Applications. Iowa St. Univ. Press, Ames, IA.

Senbayram, M., Chen, R., Budai, A., Bakken, L., Dittert, K., 2012. N2O emission and the N2O/(N2O+N2) product ratio of denitrification as controlled by available carbon substrates and nitrate concentrations. Agric. Ecosyst. Environ. 147, 4–12, http://dx.doi.org/10.1016/j.agee.2011.06.022.

Shcherbak, I., Millar, N., Robertson, G.P., 2014. Global metaanalysis of the nonlinear response of soil nitrous oxide (N2O) emissions to fertilizer nitrogen. Proc. Natl. Acad. Sci. U. S. A. 111, 9199–9204, http://dx.doi.org/10.1073/pnas.1322434111.

Šimůnek, J., Suarez, D., 1993. Modeling of carbon-dioxide transport and production in soil. 1. Model development. Water Resour. Res. 29, 487–497, http://dx.doi.org/10.1029/92WR02225.

Smith, P., Martino, D., Cai, Z., Gwary, D., Janzen, H., Kumar, P., McCarl, B., Ogle, S., O'Mara, F., Rice, C., Scholes, B., Sirotenko, O., Howden, M., McAllister, T., Pan, G., Romanenkov, V., Schneider, U., Towprayoon, S., Wattenbach, M., Smith, J., 2008. Greenhouse gas mitigation in agriculture. Philos. Trans. R. Soc. B-Biol. Sci. 363, 789–813, http://dx.doi.org/10.1098/rstb.2007.2184.

Wang, X., Williams, J.R., Gassman, P.W., Baffaut, C., Izaurralde, R.C., Jeong, J., Kiniry, J.R., 2012. Epic and apex: model use, calibration, and validation. Trans. Asabe 55, 1447–1462.

Wang, G., Mayes, M.A., Gu, L., Schadt, C.W., 2014. Representation of dormant and active microbial dynamics for ecosystem modeling. PLoS One 9, e89252, http://dx.doi.org/10.1371/journal.pone.0089252.

Wild, A., 1988. Russell's Soil Conditions and Plant Growth, 11th ed. Longman Scientific and Technical, Essex, England.

Williams, J., Jones, C., Dyke, P., 1984. A modeling approach to determining the relationship between erosion and soil productivity. Trans. ASAE 27, 129–144.

Williams, J.R., Arnold, J.G., Kiniry, J.R., Gassman, P.W., Green, C.H., 2008. History of model development at Temple, Texas. Hydrol. Sci. J.-J. Sci. Hydrol. 53, 948–960, http://dx.doi.org/10.1623/hysj.53.5.948.

Williams, J., 1990. The erosion-productivity impact calculator (epic) model – a case-history. Philos. Trans. R. Soc. Lond. Ser. B-Biol. Sci. 329, 421–428, http://dx.doi.org/10.1098/rstb.1990.0184.

Wrage, N., Velthof, G.L., van Beusichem, M.L., Oenema, O., 2001. Role of nitrifier denitrification in the production of nitrous oxide. Soil Biol. Biochem. 33, 1723–1732, http://dx.doi.org/10.1016/S0038-0717(01)00096-7.

Zhu, X., Burger, M., Doane, T.A., Horwath, W.R., 2013. Ammonia oxidation pathways and nitrifier denitrification are significant sources of N2O and NO under low oxygen availability. Proc. Natl. Acad. Sci. 110, 6328–6333, http://dx.doi.org/10.1073/pnas.1219993110.